Available online at www.sciencedirect.com

ScienceDirect

Procedia Computer Science 108C (2017) 235–244

Procedia Computer Science

International Conference on Computational Science, ICCS 2017, 12-14 June 2017, Zurich, Switzerland

Fast Motion of Heaving Airfoils

Siddhartha Verma[1], Guido Novati[1], Flavio Noca[2], and Petros Koumoutsakos[1,3,4]*

[1] Computational Science and Engineering Laboratory, ETH Zürich, CH-8092, Switzerland
[2] HEPIA (University of Applied Sciences - Western Switzerland), Geneva, Switzerland
[3] Radcliffe Institute of Advanced Study, Harvard University, MA, United States of America
[4] Wallace Visiting Professor, Massachusetts Institute of Technology, MA, United States of America

Abstract

Heaving airfoils can provide invaluable physical insight regarding the flapping flight of birds and insects. We examine the thrust-generation mechanism of oscillating foils, by coupling two-dimensional simulations with multi-objective optimization algorithms. We show that the majority of the thrust originates from the creation of low pressure regions near the leading edge of the airfoil. We optimize the motion of symmetric airfoils exploiting the Knoller-Betz-Katzmayr effect, to attain high speed and lower energy expenditure. The results of the optimization indicate an inverse correlation between energy-efficiency, and the heaving-frequency and amplitude for a purely-heaving airfoil.

Peer-review under responsibility of the scientific committee of the International Conference on Computational Science

Keywords: Flapping airfoils, multi-objective optimization, Knoller-Betz effect, Katzmayr effect

1 Introduction

Heaving and pitching airfoils have long been used for studying unsteady aerodynamics [22, 29]. These studies have been motivated primarily by curiosity regarding insect and bird flight [30, 25], and by the desire to exploit unsteady effects for practical applications at relatively low Reynolds numbers [27]. Curiously enough, oscillating airfoils that are perfectly symmetric (i.e., with no camber) have been shown to generate forward thrust with very high mechanical efficiency [2, 25]. This phenomenon, referred to as the 'Knoller-Betz-Katzmayr' effect, has aided in the development of biologically inspired MAVs (Micro Aerial Vehicles) [14]. This effect may also help windsurfers to some extent, in a technique known as 'sail-pumping' [24], which allows surfers to accelerate rapidly at low wind-speed conditions.

The aerodynamic behaviour of airfoils in a periodically-varying flow-field was first considered by Knoller [17] and Betz [4]. They showed how a perfectly symmetric airfoil undergoing pure heaving motion is capable of producing forward thrust, owing to a periodic change in the effective angle of attack. This was confirmed by Katzmayr via windtunnel experiments [16]. A theoretical analysis of the phenomenon was given by Birnbaum [5] and Garrick [9], albeit

*petros@ethz.ch

1877-0509
Peer-review under responsibility of the scientific committee of the International Conference on Computational Science
10.1016/j.procs.2017.05.166

with the limitation of small-amplitude motion, which is a necessity under the assumption of linearized quasi-steady motion. In a thrust-generating scenario, von Karman and Burgers [34] noted that the resulting wake-vortices would appear in a 'reverse' Karman vortex street pattern. For foils oscillating perpendicular to the direction of motion, dye-visualizations in water tunnels have been used to identify the dependence of thrust-generation on the Strouhal number and the angle of attack [28, 20]. Certain experimental studies have also relied on soap-films for wake-visualization of oscillating foils [23, 1]. The transition from a drag- to a thrust-producing regime is often identified as the point when the vortex-pattern in the wake switches from a regular to a reverse Karman vortex street. Such studies have also been performed numerically, using inviscid panel-vortex method [15], and using 2D [21, 35, 1] and 3D [33] Navier-Stokes solvers. Experimental studies have also been conducted for the case of pure pitching motion [8, 18], and indicate that thrust-type wakes may exist for certain oscillation angles and frequencies.

In this paper, we investigate the aerodynamic characteristics of flapping airfoils, by combining numerical simulations with multi-objective optimization algorithms. Two potentially conflicting goals, namely, the average speed and the Cost of Transport (or CoT, which measures the energy spent for travelling a unit-distance) are considered. Both these objectives are critical for the survival of most swimming and flying organisms, in addition to being extremely important metrics for gauging the performance of mechanical devices. Section 2 provides a brief description of the numerical methods used in the simulations, as well as an introduction to the multi-objective optimization algorithm used. The mechanism of thrust-generation in the case of a purely heaving airfoil is examined in Section 3.1, and results obtained via the optimization procedure are presented in Section 3.2, followed by concluding remarks in Section 4.

2 Methods

Simulation software. We use an open source fluids solver, 'MRAG-I2D' [26], to conduct numerical simulations of heaving airfoils. The code is capable of simulating two-dimensional, viscous, incompressible flows on multi-core architectures. The use of multi-resolution grids, capable of adapting automatically in both space and time, enables accurate simulations while keeping both computational cost and memory requirement low. The parallel implementation of the multi-objective optimization algorithms is based on the TORC task-parallel library [13]. TORC provides a programming and runtime environment similar to OpenMP tasks, but allows parallel programs to run on both shared and distributed memory systems. MPI applications run on the compute nodes with one or more workers, and can submit tasks for asynchronous execution from any nesting level of parallelism. TORC has already been used for the parallelization of algorithms for single objective stochastic optimization and uncertainty quantification algorithms, as part of the Π4U [12] framework.

Numerical methods. The solver used in the present study is based on the remeshed vortex methods [19], and has been validated and used extensively for simulations of complex static as well as deforming objects [10, 11, 32]. The velocity field in the simulations is governed by the incompressible Navier-Stokes equations:

$$\nabla \cdot \boldsymbol{u} = 0 \tag{1}$$

$$\frac{\partial \boldsymbol{u}}{\partial t} + (\boldsymbol{u} \cdot \nabla)\boldsymbol{u} = \frac{-\nabla P}{\rho} + \nu \nabla^2 \boldsymbol{u} \tag{2}$$

The interaction between fluid-flow and solid objects is achieved via Brinkman penalization [3], which leads to a modified form of the vorticity equation:

$$\frac{\partial \boldsymbol{\omega}}{\partial t} + (\boldsymbol{u} \cdot \nabla)\boldsymbol{\omega} = \nu \nabla^2 \boldsymbol{\omega} + \lambda \nabla \times (\chi \, (\boldsymbol{u}_s - \boldsymbol{u})) \tag{3}$$

Here, λ is a penalty parameter, and χ is the characteristic function describing the distribution of the solid object on a the Cartesian fluid-grid. The symbol $\boldsymbol{u}_s$ in Eq. 3 denotes the pointwise velocity of the discretized solid, and accounts for translation, rotation, and deformation of the body. Further details regarding spatial discretization, fluid-solid interaction, and the time-splitting steps involved in solving Eq. 3 are provided in refs. [10, 26].

Optimization objectives. There are two distinct objectives that we optimize the oscillating airfoils for, namely, maximizing the average horizontal speed, and minimizing the energy consumed for travelling a unit distance (also referred to as the Cost of Transport). The CoT is measured as the ratio of total work done for vertical and rotational oscillation of the airfoils, to the total horizontal distance travelled:

$$CoT(t) = \frac{\int_0^t (F_y u_y + \tau \dot{\alpha}) \, dt}{\int_0^t u_x dt} \tag{4}$$

Here, F_y is the negative of the flow-induced force acting on the airfoil in the vertical direction, and τ is the negative of the flow-induced torque. u_y represents the imposed sinusoidal vertical velocity, and $\dot{\alpha}$ is the imposed sinusoidal angular velocity (which is zero in the case of purely-heaving airfoils). u_x denotes horizontal velocity, which is an outcome of the interaction between the oscillating foil and the fluid-flow. The average horizontal speed and the CoT comprise the 'fitness' values used for the multi-objective optimization algorithm, which is described below.

Optimization algorithm. Evolutionary-optimization algorithms are designed to mimic the rules of evolution in biology, and involve the processes of mutation, reproduction, and selection. These strategies operate on a collection of individuals to iteratively improve the population with respect to a certain 'fitness' value, which represents the eligibility of a particular individual to pass on its characteristics to future generations. The particular algorithm that we use in this study is referred to as the Non-dominated Sorting Genetic Algorithm II (NSGA-II) [7]. This algorithm improves on the original NSGA [31] by introducing elitism, the crowding distance parameter, and a fast non-dominated sorting algorithm. A description of the NSGA-II procedure is provided in Algorithm 1. The crossover step of the algorithm is performed using Simulated Binary Crossover (SBX), whereas Parameter-based Mutation (PBM) is used for the mutation step [6].

3 Results

3.1 Dynamics of a Purely Heaving Airfoil

In this section, we examine the dynamics of an airfoil undergoing a pure heaving motion. A sinusoidal velocity is imposed on a NACA0012 airfoil in the vertical direction, and the angle of attack is held fixed at zero ($\alpha = 0$). The goal is to provide a more detailed understanding of flow-induced thrust generation, than is possible by examining the reverse von Karman street, or by examining the momentum excess/deficiency in the wake.

Algorithm 1: NSGA-II

Initialize population $P^{(0)}$ of size μ and set generation $g = 0$.
while *No stopping criterion is met* **do**
  Generate an offspring population $\bar{P}^{(g+1)}$ from the parent population $P^{(g)}$ using crossover and mutation.
  Combine offspring $\bar{P}^{(g+1)}$ and parent population $P^{(g)}$ into a mixed population and sort it according to non-domination rank and crowding distance.
  Select the best μ individuals for the next parent generation $P^{(g+1)}$.
  $g = g + 1$
end
Output the current population.

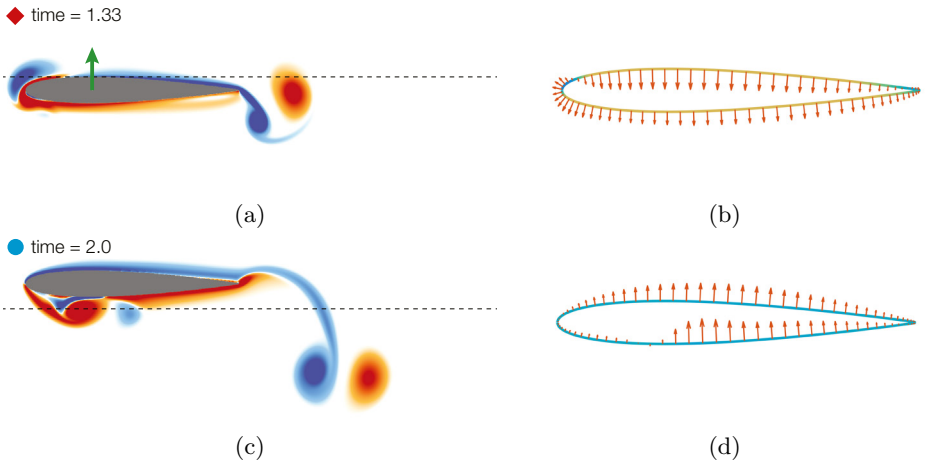

Figure 1: (a, c) Vorticity contours around an airfoil oscillating with a heave-amplitude of 0.12L (where L is the chord length), and a heave-frequency of 0.5Hz. The vorticity-field is shown at two time-instances during initial speed-up. The solid green arrow in (a) indicates the direction of motion of the airfoil. (b, d) The corresponding fluid-induced force distribution on the airfoil surface.

Figure 1 shows the vorticity-field generated by the oscillating airfoil at two points in time during initial acceleration, along with the flow-induced force-distribution on the airfoil's surface. The corresponding time-series plots showing the variation of airfoil speed, flow-induced force, power input, and the CoT are provided in Fig. 2. We note that all the airfoils described in this study start from rest, and there is no inflow imposed at any time. At $t = 1.33$, the airfoil is moving vertically upward with high velocity, as illustrated by the u_y curve in Fig. 2a (red diamond). The resulting fluid-induced force impedes this motion (negative F_y, Fig. 2b), and leads the imposed u_y by a phase angle of $\pi/2$ throughout the simulation. A large amount of work is put into moving the airfoil at this instance, as indicated by the positive peak in Fig. 2c. Interestingly, this gives rise to very large forward thrust, as can be surmised from the positive peak in F_x (Fig. 2b). The origin of this thrust is evident in Figs. 1a and 1b; the vortices shed near the leading edge (Fig. 1a) generate a low pressure region, which gives rise to horizontal acceleration-forces (Fig. 1b) on the airfoil's surface.

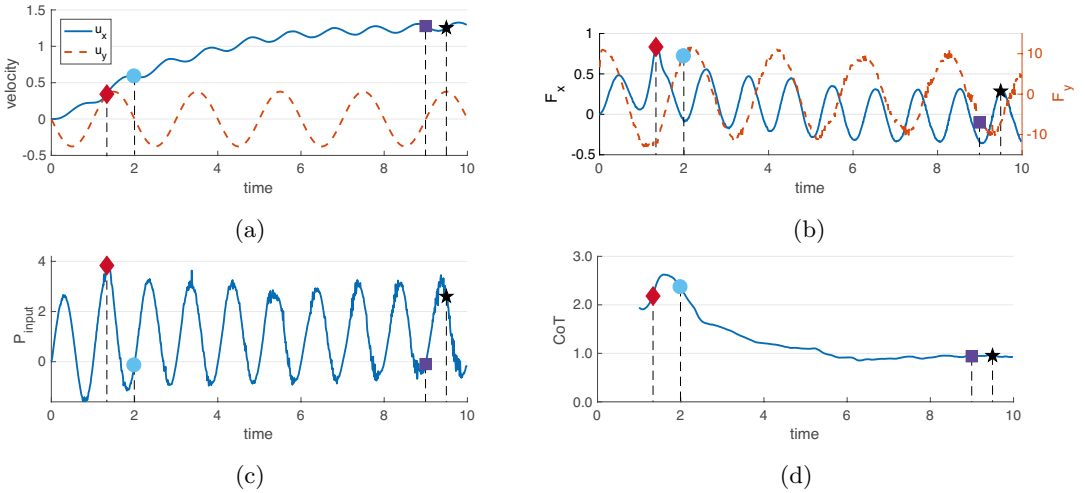

Figure 2: The time-variation of (a) horizontal and vertical speed, (b) horizontal and vertical (dashed line, secondary y-axis) flow-induced force, (c) the power required for airfoil-oscillations, and (d) the CoT computed at any particular instance as work/distance over the previous time period.

The next instance we examine, at $t = 2.0$, corresponds to zero forward-thrust on the airfoil. At this point, the airfoil has come to a vertical stop ($u_y = 0$), and vortex-shedding occurs aft of the leading edge (Fig. 1c). The resulting low-pressure region reduces the net vertical fluid-induced force, but there is no assistance to the forward motion of the airfoil ($F_x = 0$ in Fig. 2b). Practically all the force-vectors in Fig. 1d point in the vertical direction. We remark that the temporal frequency associated with u_x and F_x in Figs. 2a and 2b, is twice the imposed frequency of the airfoil (which is the same as the frequency of u_y and F_y). This is expected, since the symmetric airfoil encounters the same absolute conditions every half a period of the vertical oscillation (except during initial startup), but with the opposite sign.

As the simulation progresses, the increasing speed of the airfoil gives rise to higher viscous- and pressure-drag. The airfoil keeps speeding up, until the thrust force generated by the Katzmayr effect is balanced by drag forces (around $t = 8.0$ in Fig. 2a). Beyond this point, the mean F_x and F_y values approach zero (Fig. 2b), and the airfoil maintains a steady mean speed. The CoT also approaches a steady value (Fig. 2d), which is smaller than the transient values measured during the start-up phase. We examine two particular instances during this steady phase, corresponding to maximum thrust ($t = 9.0$) and maximum drag ($t = 9.5$) experienced by the airfoil. The relevant flow-field and the surface force-distributions are shown in Fig. 3. At $t = 9.0$, the airfoil reaches its maximum oscillation displacement, and stops moving vertically. At this point, the flow is mainly head-on with respect to the airfoil (i.e., zero angle of attack), which gives rise to drag force at the leading edge (force vectors pointing aft - Fig. 3b). Meanwhile, the airfoil attains its maximum upward speed at $t = 9.5$, and a low pressure region forms on the lower surface near the leading edge. The gives rise to acceleration-inducing forces, as can be seen in Fig. 3d (force vectors pointing-forward).

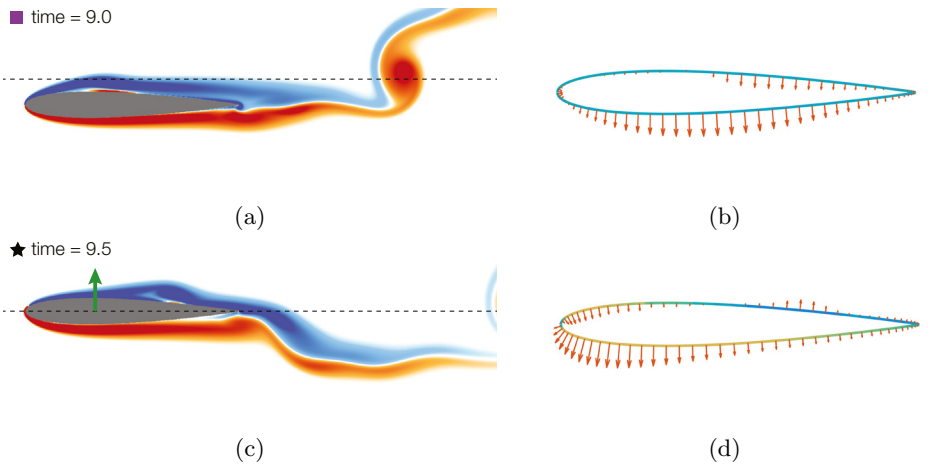

Figure 3: (a, c) Vorticity contours around the airfoil at $t = 9.0$ and $t = 9.5$. (b, d) The corresponding fluid-induced force-distribution. The solid green arrow in (c) indicates the direction of motion of the airfoil.

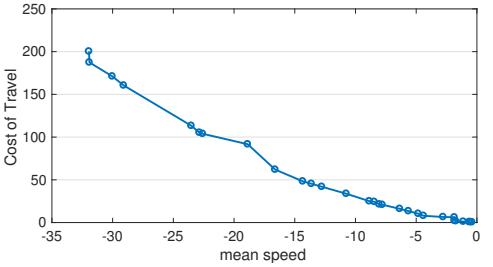

Figure 4: Pareto front obtained for an airfoil in pure-heaving motion.

3.2 Optimal Heaving Motion

In this section, we will discuss the optimal oscillatory motion discovered by the optimization algorithm. A purely-heaving motion is considered, with the optimization parameters being the heave amplitude (A_h) and frequency (f_h). The Pareto front, which depicts the tradeoff between speed and CoT amongst the fittest individuals found by the optimization algorithm, is shown in Fig. 4. We clearly observe that faster individuals (which correspond to increasingly negative speed, since the optimization algorithm acts as minimizer) tend to incur a significantly higher cost for travelling a unit distance. On the other hand, the individuals attempting to minimize CoT tend to be extremely slow. A compromise between speed and CoT may be reached by selecting an individual which shows a balanced performance with respect to both these quantities. The performance of various optimal individuals is discussed below.

To inspect the impact of optimization on aerodynamic performance, we select three distinct individuals from the Pareto front in Fig. 4, one from either extreme (i.e., maximum speed, and maximum CoT), and one with intermediate values for both speed and CoT (a 'generalist' foil). The time-varying horizontal speeds and CoT of these three individuals are compared in Fig. 5. We observe that the fastest individual dominates the other two in terms of speed (Fig. 5a), but requires approximately 2 orders of magnitude more energy than the generalist foil, and 3

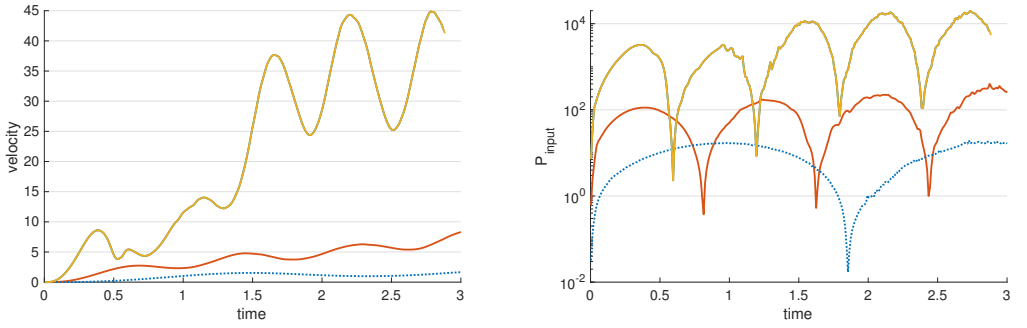

(a) (b)

Figure 5: (a) Instantaneous horizontal speed , and (b) power input for the three relevant airfoils undergoing pure heaving motion. The data for the fastest foil is shown using the solid yellow line, for the generalist foil using the dashed orange line, and that for the most efficient foil using the dotted blue line.

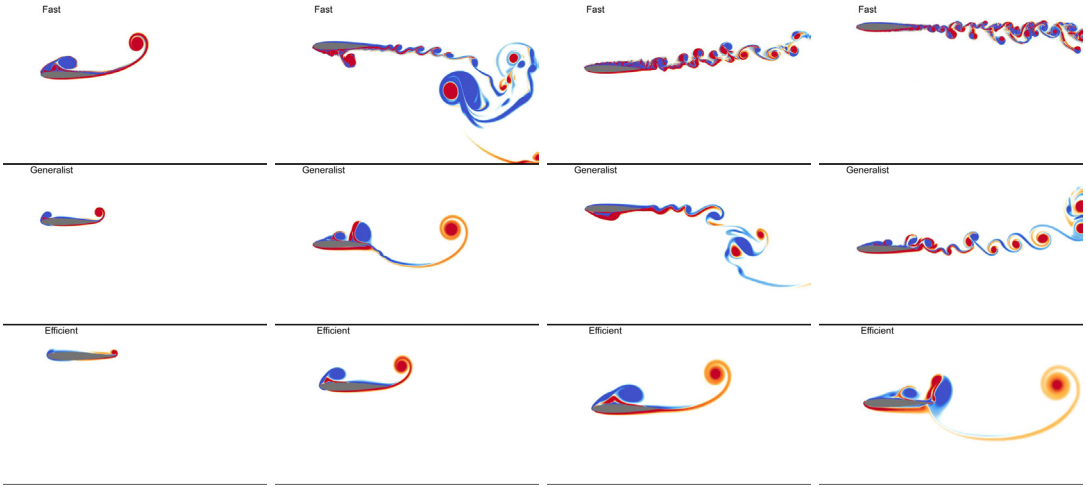

(a) (b) (c) (d)

Figure 6: Vorticity-field generated by the optimal airfoils at various time instances. The fastest airfoil is shown in the top row, the generalist in the middle, and the most efficient airfoil is shown in the bottom row.

orders more than the efficient one (Fig. 5b). The corresponding flow-fields generated by these individuals are shown in Fig. 6, and in supplementary Movie 1.

In Fig. 7, we examine how the two optimization-parameters, A_h and f_h, vary for the individuals lying on the Pareto front. The individuals are arranged in order of increasing efficiency, such that individual 1 is the least efficient, but the fastest one. We observe that the fast individuals tend to employ larger heaving amplitudes, with the value of A_h decreasing steadily from approximately 0.9 chord lengths to 0.5, for more efficient individuals. Similarly, the heaving frequency decreases from approximately 0.6 Hz to 0.1 Hz. The results indicate that airfoils must oscillate faster and with larger amplitudes to generate increased thrust via the Katzmayr

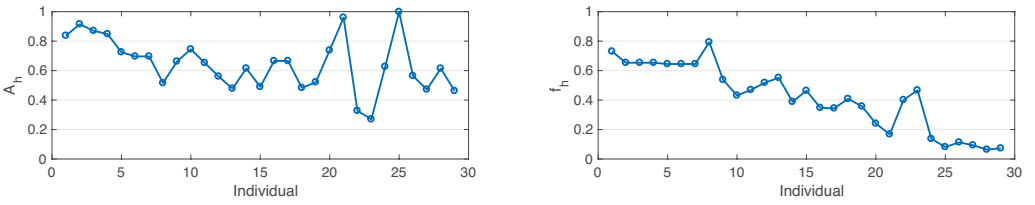

(a) (b)

Figure 7: (a) The heaving amplitude normalized by the chord length of the foil, and (b) the heaving frequency shown in Hz.

effect, but at the expense of much higher energy expenditure.

4 Conclusion

We have analyzed the motion of flapping airfoils with the help of numerical simulations combined with multi-objective optimization. We investigated the dynamics of a symmetric airfoil undergoing pure heaving motion, to examine the mechanism of thrust-generation via the Katzmayr effect. We discovered that the majority of the thrust originates from the creation of low pressure regions near the leading edge of the airfoil. We then identified the optimal heaving amplitude and frequency for attaining two potentially conflicting objectives, namely high speed and low energy expenditure, with the help of optimization algorithms. The results indicate that airfoils must oscillate faster and with larger amplitudes to generate increased thrust via the Katzmayr effect, but at the expense of much higher energy expenditure. It may be feasible to reduce energetic costs by using a judicious combination of heaving and pitching motion, which will be a subject for future investigation. We expect that the results provided here will serve as a starting point for investigating the physics of optimal flapping flight in birds and insects.

Acknowledgments

This work was supported by the European Research Council Advanced Investigator Award (341117), and the SNSF Sinergia Award (CRSII3 147675). Computational resources were provided by the Swiss National Supercomputing Center (CSCS) under project ID ‘s658’.

References

[1] A. Andersen, T. Bohr, T. Schnipper, and J. H. Walther. Wake structure and thrust generation of a flapping foil in two-dimensional flow. *Journal of Fluid Mechanics*, 812, 002 2017.

[2] J. M. Anderson, K. Streitlien, D. S. Barrett, and M. S. Triantafyllou. Oscillating foils of high propulsive efficiency. *Journal of Fluid Mechanics*, 360:41–72, April 1998.

[3] P. Angot, C. H. Bruneau, and P. Fabrie. A penalization method to take into account obstacles in incompressible viscous flows. *Numer. Math.*, 81:497–520, 1999.

[4] A. Betz. Ein beitrag zur erklaerung des segelfluges. *Zeits. Flug. .Motorluft.*, 3:269–270, 1912.

[5] W. Birnbaum. Das ebene problem des schlagenden flgels. *ZAMM - Journal of Applied Mathematics and Mechanics / Zeitschrift fr Angewandte Mathematik und Mechanik*, 4(4):277–292, 1924.

[6] K. Deb and S. Agrawal. *A Niched-Penalty Approach for Constraint Handling in Genetic Algorithms*, pages 235–243. Springer Vienna, Vienna, 1999.

[7] K. Deb, A. Pratap, S. Agarwal, and T. Meyarivan. A fast and elitist multi-objective genetic algorithm: NSGA-II, 2000.

[8] P. Freymuth. Propulsive vortical signature of plunging and pitching airfoils. *AIAA Journal*, 26(7):881–883, 2017/02/09 1988.

[9] I. E. Garrick. Propulsion of a flapping and oscillating airfoil. *NACA*, 567, 1936.

[10] M. Gazzola, P. Chatelain, W. M. van Rees, and P. Koumoutsakos. Simulations of single and multiple swimmers with non-divergence free deforming geometries. *J. Comput. Phys.*, 230, 2011.

[11] M. Gazzola, Wim M. van Rees, and P. Koumoutsakos. C-start: optimal start of larval fish. *Journal of Fluid Mechanics*, 698:5–18, May 2012.

[12] P. E. Hadjidoukas, P. Angelikopoulos, L. Kulakova, C. Papadimitriou, and P. Koumoutsakos. Exploiting task-based parallelism in bayesian uncertainty quantification. In *European Conference on Parallel Processing*, pages 532–544. Springer, 2015.

[13] P. E. Hadjidoukas, E. Lappas, and V. V. Dimakopoulos. A runtime library for platform-independent task parallelism. In *2012 20th Euromicro International Conference on Parallel, Distributed and Network-based Processing*, pages 229–236. IEEE, 2012.

[14] K. D. Jones and M. F. Platzer. Design and development considerations for biologically inspired flapping-wing micro air vehicles. *Experiments in Fluids*, 46(5):799–810, 2009.

[15] K. Kamemoto and T. Mine. *Calculation of Aerodynamic Characteristics of a Heaving and Pitching Airfoil by a Panel-Vortex Method*. Springer Berlin Heidelberg, Berlin, Heidelberg, 1992.

[16] R. Katzmayr. Effect of periodic changes of angle of attack on behaviour of airfoils. *NACA*, 1922.

[17] R. Knoller. Die gesetze des luftwiderstandes. *Flug- und Motortechnik*, 3:1–7, 1912.

[18] M. M. Koochesfahani. Vortical patterns in the wake of an oscillating airfoil. *AIAA J.*, 27, 1989.

[19] P. Koumoutsakos and A. Leonard. High-resolution simulations of the flow around an impulsively started cylinder using vortex methods. *J. Fluid Mech.*, 296:1–38, 1995.

[20] T. C. W. Lau, R. M. Kelso, and E. R. Hassan. Flow visualisation of a pitching and heaving hydrofoil. In *15th Australasian Fluid Mechanics Conference*, 2004.

[21] G. C. Lewin and H. Haj-Hariri. Modelling thrust generation of a two-dimensional heaving airfoil in a viscous flow. *Journal of Fluid Mechanics*, 492:339–362, 10 2003.

[22] W. J. McCroskey. Unsteady airfoils. *Annual Review of Fluid Mechanics*, 14(1):285–311, 1982.

[23] F. T. Muijres and D. Lentink. Wake visualization of a heaving and pitching foil in a soap film. *Experiments in Fluids*, 43(5):665–673, 2007.

[24] N. Ouadahi, A. Ababou, N. Ababou, and M. A. Larbi. Windsurf ergometer for sail pumping analysis and mechanical power measurement. *Procedia Engineering*, 72:249 – 254, 2014.

[25] D. A. Read, F. S. Hover, and M. S. Triantafyllou. Forces on oscillating foils for propulsion and maneuvering. *Journal of Fluids and Structures*, 17(1):163 – 183, 2003.

[26] D. Rossinelli, B. Hejazialhosseini, W. M. van Rees, M. Gazzola, M. Bergdorf, and P. Koumoutsakos. MRAG-I2D: Multi-resolution adapted grids for remeshed vortex methods on multicore architectures. *J. Comput. Phys.*, 288:1–18, 2015.

[27] K. V. Rozhdestvensky and V. A. Ryzhov. Aerohydrodynamics of flapping-wing propulsors. *Progress in Aerospace Sciences*, 39(8):585 – 633, 2003.

[28] J. C. S. Lai and M. F. Platzer. Jet characteristics of a plunging airfoil. *AIAA J.*, 37(12), 1999.

[29] W. Shyy, H. Aono, S.K. Chimakurthi, P. Trizila, C.-K. Kang, C.E.S. Cesnik, and H. Liu. Recent progress in flapping wing aerodynamics and aeroelasticity. *Prog. Aero. Sci.*, 46, 2010.

[30] W. Shyy, Y. Lian, J. Tang, D. Viieru, and H. Liu. *Aerodynamics of Low Reynolds Number Flyers:*. Cambridge University Press, Cambridge, 10 2007.

[31] N. Srinivas and K. Deb. Muiltiobjective optimization using nondominated sorting in genetic algorithms. *Evol. Comput.*, 2(3):221–248, September 1994.

[32] W. M. van Rees, M. Gazzola, and P. Koumoutsakos. Optimal shapes for anguilliform swimmers

at intermediate reynolds numbers. *J. Fluid Mech.*, 722, 5 2013.

[33] M. Visbal, T. O. Yilmaz, and D. Rockwell. Three-dimensional vortex formation on a heaving low-aspect-ratio wing: Computations and experiments. *J. Fluids. Struct.*, 38:58 – 76, 2013.

[34] T. von Karman and J. Burgers. *General aerodynamic theory-perfect fluids*. Springer-Verlag, 1934.

[35] J. Young and J. C. S. Lai. Mechanisms influencing the efficiency of oscillating airfoil propulsion. *AIAA J.*, 45(7):1695–1702, 2007.